A new predictive dynamic model describing the effect of the ambient temperature and the convective heat transfer coefficient on bacterial growth

Hana Ben Yaghlene, Ivan Leguérinel, Moktar Hamdi, Pierre Mafart

A new predictive dynamic model describing the effect of the ambient temperature and the convective heat transfer coefficient on bacterial growth

H. Ben Yaghlene[a,b*], I. Leguerinel[a], M. Hamdi[b], P. Mafart[a]

[a] : Université Européenne de Bretagne, EA3882, Laboratoire Universitaire de Biodiversité et Ecologie Microbienne, IFR148 ScInBioS, Université de Bretagne Occidentale, 6 rue de l'université, F29334 Quimper, Cedex, France

[b] : Laboratoire d'Ecologie et de Technologie Microbienne, Institut National des Sciences Appliquées et de Technologie (INSAT), 2 Boulevard de la terre, B.P. 676, 1080 Tunis, Tunisie

[*]Corresponding author: LUBEM, UBO, 6 rue de l'Université, F29334, Quimper Cedex, France. Tel.: +33 2 98 90 02 27; Fax: +33 2 98 90 85 44

E mail address: hana.benyaghlene@univ-brest.fr

Abstract

In this study, predictive microbiology and food engineering were combined in order to develop a new analytical model predicting the bacterial growth under dynamic temperature conditions. The proposed model associates a simplified primary bacterial growth model without lag, the secondary Ratkowsky "square root" model and a simplified two-parameter heat transfer model regarding an infinite slab. The model takes into consideration the product thickness, its thermal properties, the ambient air temperature, the convective heat transfer coefficient and the growth parameters of the micro organism of concern. For the validation of the overall model, five different combinations of ambient air temperature (ranging from 8 °C to 12 °C), product thickness (ranging from 1 cm to 6 cm) and convective heat transfer coefficient (ranging from 8 W/(m^2.K) to 60 W/(m^2.K)) were tested during a cooling

27 procedure. Moreover, three different ambient air temperature scenarios assuming alternated

28 cooling and heating stages, drawn from real refrigerated food processes, were tested. General

29 agreement between predicted and observed bacterial growth was obtained and less than 5% of

30 the experimental data fell outside the 95 percent confidence bands estimated by the bootstrap

31 percentile method, at all the tested conditions. Accordingly, the overall model was

32 successfully validated for isothermal and dynamic refrigeration cycles allowing for

33 temperature dynamic changes at the centre and at the surface of the product. The major

34 impact of the convective heat transfer coefficient and the product thickness on bacterial

35 growth during the product cooling was demonstrated. For instance, the time needed for the

36 same level of bacterial growth to be reached at the product's half thickness was estimated to

37 be 5 and 16.5 h at low and high convection level, respectively. Moreover, simulation results

38 demonstrated that the predicted bacterial growth at the air ambient temperature cannot be

39 assumed to be equivalent to the bacterial growth occurring at the product's surface or centre

40 when convection heat transfer is taken into account. Our results indicate that combining food

41 engineering and predictive microbiology models is an interesting approach providing very

42 useful tools for food safety and process optimisation.

43

44 **Key words:**

45 Predictive microbiology; Heat transfer; Dynamic models; Bacterial growth; Cooling; Heating.

2

Nomenclature

46   **Nomenclature**

47

A	Transfer area (m^2)
Bi	Biot number
E	Product thickness (m)
f'	Thermal proliferation value
Fo	Fourier number
h	Convective heat transfer coefficient ($W/(m^2.K)$)
j	Lag factor for reduced temperature profile
k	Slope of the linear portion of the semi-logarithmic plot of reduced temperature *vs* time.
l	Characteristic dimension (m)
N	Microbial cell density at time t (CFU/mL)
N_0	Initial microbial cell density (CFU/mL)
O	Observed microbial cell density ($\log_{10}$ CFU/mL)
OD	Microbial optical density at time t
OD_0	Initial microbial optical density
P	Predicted microbial cell density ($\log_{10}$ CFU/mL)
t	Time (s)
T	Temperature of the product (°C)
T_{eq}	Equivalent temperature
T_{min}	Temperature below which no microbial growth occurs (°C)
T_{opt}	Temperature at which the microbial growth is optimal (°C)
T_0	Initial product temperature (°C)
T_∞	Ambient temperature (°C)
x	Distance from the centre (m)
x_{max}	Half-thickness for an infinite slab (m)
α	Thermal diffusivity of the product (m^2/s)
Γ	Overall gamma function
γ	Thermal gamma function
λ	Thermal conductivity of the product (W/(m.K))
μ	Specific microbial growth rate (h^{-1})
μ_{opt}	Optimal specific microbial growth rate (h^{-1})
φ	First root of $\cot \varphi = \varphi / Bi$
φ_n	Roots of $\cot \varphi = \varphi / Bi$

48

1. Introduction

50 Predictive food microbiology involves knowledge of microbial growth responses to

51 environmental factors expressed in quantitative terms by mathematical equations (models)

52 (McMeekin et al., 1997). It is generally agreed that the most important environmental factor

53 that affects bacterial growth in food is temperature. This factor is constantly changing during

54 processing, storage and distribution of food products (Fujikawa et al., 2004). At the same

55 time, control organizations propose stringent requirements regarding monitoring of the

56 internal temperature of products being processed. For instance, according to the United States

57 Department of Agriculture, the allowable growth of *Clostridium perfringens* during the

58 cooling of certain meat and poultry products should be limited to 1 log (U.S.D.A, 1999). In

59 the case of cured products, the guidelines recommend that products' internal temperature

60 should be reduced from 54.4 °C to 26.6 °C in less than 5 h, and from 26.6 °C to 7.2 °C in the

61 next 10 h (15 h total cooling time).

62 Predictive microbiology is a useful tool for assessing and controlling food safety particularly

63 when models are able to cope with dynamic conditions such as changing temperatures.

64 Numerous published models, reported in Table 1, have dealt with the prediction of bacterial

65 growth under dynamic temperature conditions. Generally, these works were based on

66 predictive models corresponding to isothermal bacterial growths which were modified in

67 order to consider the effect of temperature changes. These studies primarily aimed at

68 assessing the feasibility of predicting the bacterial growth at changing temperature. Indeed,

69 predicting bacterial growth under dynamic conditions has been shown to be possible via the

70 dynamic transformation of existing static models. According to the authors of the cited studies

71 (Table 1), the models' predictions agreed well with experimental results after temperature

72 changes.

73   Nevertheless, the considered scenarios of changing temperatures within bacterial models were

74   various. In some cases, typical temperature profiles were considered either by the use of

75   hypothetical ones or by the adoption of real temperature scenarios recorded while the studied

76   products had been processed. In other cases, temperature profiles were simulated from heat

77   transfer models. Mathematical models that integrate effectively heat transfer phenomena and

78   dynamic bacterial growth relationships are scarce (Amezquita et al., 2005; de Jong et al.,

79   2005; Zwietering and Hasting, 1997). Armitage (1997) derived the temperature histories for

80   the deep leg and leg surface of a lamb carcass by using finite element models for dealing with

81   regular shapes. Temperature function integration technique (TFI) was applied to the

82   calculated temperature histories of five different cooling processes to simulate *Escherichia*

83   *coli* growth on the leg surface of each carcass during aging. TFI technique was previously

84   introduced by Gill and Harrison (1985). Data related to the growth of six strains of *E. coli*

85   isolated from commercially packed livers were fitted according to the Ratkowsky model

86   (Ratkowsky et al., 1982) linking the growth rate to temperature. Total growth was obtained by

87   summation of partial growth calculated within sequential 3.75-min periods from the growth

88   rate for the average temperature within each period. Estimated bacterial growth during offals

89   cooling (cooling profiles were directly recorded on several offals being chilled) agreed well

90   with observed data with *E. coli*. Bellara et al. (2000) experimentally validated bacterial

91   growth modelling involving a heat transfer model of temperature fluctuations within a solid

92   object. From data related to *E. coli* W3110 growth in agar, a model was set up describing

93   bacterial growth as a function of temperature. This was then used in conjunction with a finite

94   difference heat transfer model describing temperature change in a cylinder in order to

95   calculate the bacterial growth that occurs in agar gel inside a cylindrical glass vessel under

96   conduction cooling. Excellent agreement was found between model simulations and

97   experimental data. Alavi et al. (2001) determined the growth characteristics of *Listeria*

98   *monocytogenes* in sterilized whole milk. The parameter values of the Baranyi dynamic growth

99   model (Baranyi et al., 1995) were determined. Finite element software, ANSYS, was

100   implemented to determine temperature distributions in milk cartons subject to a time-varying

101   ambient temperature profile. The space-time-temperature data were input to the Baranyi

102   dynamic growth model, to predict the microbial population density distribution and the

103   average population density in the milk carton. Amezquita et al. (2005) developed a computer

104   simulation scheme to analyze heat transfer phenomena and temperature-dependent *C.*

105   *perfringens* growth during cooling of cooked boneless cured ham. The temperature history of

106   ham was predicted from a finite element heat diffusion model. For *C. perfringens* growth, a

107   dynamic model was developed from the Baranyi's nonautonomous differential equation

108   (Baranyi and Roberts, 1994). The bacterium's growth model was integrated into the computer

109   program taking predicted temperature histories as input values. Validation of the model

110   predictions considered three different time–temperature cooling histories from 54.4 °C to 7.2

111   °C of the geometrical centre of a large cooked boneless ham. In a further work (Corradini et

112   al., 2006), the same data were fitted with the ad hoc empirical models in order to define the

113   three parameters temperature dependence of the modified version of the logistic primary

114   model. The continuous rate equation was solved incrementally by a numerical procedure

115   implemented in general purpose software. In both Amezquita et al. (2005) and Corradini et al.

116   (2006) works, predicted *C. perfringens* growth curves obtained from dynamic modelling

117   showed good agreement with observed results for the tested cooling scenarios. The integrated

118   modelling approach for predicting microbial behaviour during processing was reviewed by

119   Lebert and Lebert (2006).

120   Combination of predictive microbiology and food engineering allows both the assessment of a

121   process in relation to risk and its optimisation (Mafart, 2005). In spite of all the advances

122   made in modelling microbial growth, proposing and improving new overall models which

123 combine predictive microbiology and heat transfer phenomena is an obvious necessity. The

124 more simple the proposed models and the more realistic the considered conditions are, the

125 easiest is their implementation to food processes.

126 In the present study, we aimed to develop a new analytical model combining bacterial growth

127 prediction and food engineering. Our goal was for the overall model to be simple and robust,

128 with minimum involved parameters, and to integrate the process conditions. The proposed

129 model is the association of three equations: a simplified primary model consisting of a simple

130 exponential growth equation without lag time, the Ratkowsky "square root" model linking the

131 specific growth rate to temperature (Ratkowsky et al., 1982), and a simplified two-parameter

132 heat transfer model regarding an infinite slab. While classical models assume that ambient

133 temperature is immediately reached at the growth medium, this work takes into account, not

134 only the air temperature, but also the thickness of the medium, its thermal properties and the

135 convective heat transfer coefficient. In addition, the proposed model may be easily

136 implemented to various micro organisms having known growth parameters.

137 **2. Development of the model**

138 **2.1. Heat transfer modelling**

139 All cooling processes for solid materials exhibit similar behaviour. After an initial 'lag', the

140 reduced temperature at the thermal centre of the food item decreases exponentially. The linear

141 portion of the cooling curve (obtained by plotting, on semi-logarithmic axes, the reduced

142 temperature $(T_\infty - T)/(T_\infty - T_0)$ versus time (Becker and Fricke, 2004), see Fig. A1 in the

143 appendix) can typically be described by the simplified linear asymptotic form of the general

144 heat transfer model, valid for Fourier number $Fo \geq 0.2$ with $Fo = \alpha \cdot t / l^2$ where α is thermal

145 diffusivity of the product, l is the characteristic dimension of the product, T is the local

146 temperature of the product at the time t, T_0 is the initial temperature of the product, T_∞ is the

147   cooling medium temperature (pulsed air). Consequently, the heating or cooling kinetic is

148   expressed as follows:

149 $$T = T_\infty \left(1 - je^{-kt}\right) + T_0\, je^{-kt} \qquad (1)$$

150   Where j is the lag factor and k is the slope of the linear portion of the semi-logarithmic plot of

151   reduced temperature vs time. The value of the parameter k depends upon the product shape, l,

152   α and the Biot number $Bi = hl/\lambda$, where h is the convective heat transfer coefficient between

153   the product surface area and the ambient air and λ is the thermal conductivity of the product.

154   A low Biot number ($Bi < 0.1$) indicates that the internal resistance to heat transfer is

155   negligible, and thus, the temperature within the object is uniform at any given instant in time

156   while the external thermal resistance can be neglected for $Bi > 40$ (Mafart, 1997).

157   The governing differential equation for infinite slab is given as follows with the initial

158   (uniform distribution of temperature) and boundary condition (surface convection):

159 $$\frac{\partial T}{\partial t} = \alpha \frac{\partial^2 T}{\partial x^2} \qquad (2)$$

160   where x is distance from the centre. For initial condition of uniform temperature and boundary

161   conditions of central symmetry and convective heat transfer at the surface, solution for Eq. (2)

162   is supplied by the infinite series given by Carslaw and Jaeger (1986) (see Eq. (20) in the

163   appendix). It is a general knowledge that use of the first term of this series would be enough

164   when the Fourier number is greater than 0.2 since the temperature change after that certain

165   time would be linear (Becker and Fricke, 2004; Bimbenet et al., 2002; Caro-Corrales et al.,

166   2002; Dincer, 1996; Erdogdu, 2005). As long as the thermal diffusivity is constant, this first

167   term approach may be easily used to determine the temperature change with Eq. (1) and with

168   the known heat transfer coefficient value:

169     $k = \varphi^2 . \alpha / l^2$ at any given position in the infinite slab where φ is the first root of the following

170   equation:

171
$$\cot \varphi = \frac{\varphi}{Bi} \qquad (3)$$

172 At the half thickness of the infinite slab,

173
$$j = \frac{2 \sin \varphi}{\varphi + \sin \varphi \cos \varphi} \qquad (4a)$$

174 At the surface of the infinite slab,

175
$$j = \frac{2 \sin \varphi \cos \varphi}{\varphi + \sin \varphi \cos \varphi} \qquad (4b)$$

176 With respect to the cooling/heating of the product during the initial 'lag' period ($Fo < 0.2$), we

177 assumed a straight linear link between T_0 and temperature at time corresponding to $Fo = 0.2$.

178 **2.2. Bacterial growth modelling**

179 As a primary model, a simple exponential growth without lag time was assumed:

180
$$N = N_0 e^{\mu t} \qquad (5)$$

181 Where N is the cell number at time t, N_0 is the initial cell number and μ the specific bacterial

182 growth rate at time t.

183 The gamma function corresponds to a comparison between the growth rate of microbial cells

184 growing at given environmental conditions and the optimum growth rate that would be

185 measured at optimal conditions (Zwietering et al., 1992):

186
$$\Gamma = \frac{\mu}{\mu_{opt}} \qquad (6)$$

187 In the framework of standard calculations aiming to compare processes to each others, a

188 simplified gamma function depending only on temperature can be derived from the "square

189 root" model of Ratkowsky et al. (1982) modified by Zwietering et al. (1992)

190
$$\gamma(T) = \left(\frac{T - T_{\min}}{T_{opt} - T_{\min}} \right)^2 \qquad (7)$$

9

191   Where T_{min} is the temperature below which no microbial growth occurs and T_{opt} is the

192   temperature at which the microbial growth is optimal.

193   If a process has to be intrinsically assessed regardless of the characteristics of the foodstuff, a

194   partial proliferation value may be involved. If the local temperature at which the bacteria are

195   growing is the single considered factor, Mafart (2005) defined a "thermal proliferation value"

196   as:

197
$$f' = \int_0^t \gamma(T)\, dt \qquad (8)$$

198   This value has the dimension of a time and corresponds to a time-temperature cycle that

199   would yield the same proliferation ratio than a growth of f' units of time at the optimal and

200   constant temperature (Mafart, 2005).

201   The original differential form of equation (6) is:

202
$$\frac{1}{N}\frac{d(N)}{dt} = \mu(t) = \mu_{opt}\,\gamma[T(t)] \qquad (9)$$

203   the solution of which yields:

204
$$\frac{N}{N_0} = \exp\left[\mu_{opt}\int_0^t \left(\frac{T - T_{min}}{T_{opt} - T_{min}}\right)^2 dt\right] \qquad (10)$$

205   This model can be easily combined with heat transfer models permitting the obtainment of an

206   analytic solution yielding the overall model. Note that, even for complex foodstuff shapes, an

207   analytic solution of the model is possible, provided that thermal parameters of equation (1) (j

208   and k) can be empirically determined from a temperature registration and a linear regression

209   of reduced temperature.

210   The concept of thermal proliferation value may be usefully completed by that of equivalent

211   temperature, which corresponds to the constant temperature that would yield the same

212   proliferation during the duration of a thermal cycle. A cooling/heating process can then be

213   characterised and be compared with others by its duration and its equivalent temperature

214   (Mafart, 2005).

$$\gamma\!\left(T_{eq}\right)t = f'$$ (11)

216   where time is expressed in hours. The combination of this last equation with Eq. (7) yields:

$$T_{eq} = T_{min} + \left(T_{opt} - T_{min}\right)\sqrt{\frac{f'}{t}}$$ (12)

2.3. Overall model

219   The overall model developed in the present study aims to consider the convective heat

220   transfer coefficient and the temperature of the ambient medium when predicting bacterial

221   growth under dynamic conditions of temperature.

222   Combining Eqs. (1) and (7) the obtained time-dependent $\gamma(T)$ function is employed in Eq. (8)

223   in order to express, by integration, f' as a function of t:

$$f'(T) = \frac{k\left(T_{\infty} - T_{min}\right)^2 t + 2j\left(T_{\infty} - T_{min}\right)\left(T_0 - T_{\infty}\right)\left(1 - e^{-kt}\right) + \dfrac{j^2}{2}\left(T_0 - T_{\infty}\right)^2\left(1 - e^{-2kt}\right)}{k\left(T_{opt} - T_{min}\right)^2}$$ (13)

225   The substitution of f' in Eq. (13) by its above-cited expression enables the calculation of the

226   equivalent temperature as follows:

$$T_{eq} = T_{min} + \sqrt{\frac{k\left(T_{\infty} - T_{min}\right)^2 t + 2j\left(T_{\infty} - T_{min}\right)\left(T_0 - T_{\infty}\right)\left(1 - e^{-kt}\right) + \dfrac{j^2}{2}\left(T_0 - T_{\infty}\right)^2\left(1 - e^{-2kt}\right)}{kt}}$$ (14)

228   The implementation of the Eq. (10) to T_{eq} of the thermal process yields:

$$\frac{N}{N_0} = \exp\!\left[\mu_{opt}\left(\frac{T_{eq} - T_{min}}{T_{opt} - T_{min}}\right)^2 t\right]$$ (15)

230   The overall mathematical model corresponds to the association of these two last equations.

231   The determination of the j value at the centre (Eq. (4a)) or at the surface (Eq. (4b)) of an

232   infinite slab allows the calculation of the corresponding T_{eq} values. The parameter k is

233 determined from Eq. (3) at any given position in the product and with *Bi* which includes the

234 convective heat transfer coefficient *h* that will be changed in the experimental validation of

235 the overall model.

236

237 **3. Materials and methods**

238 **3.1. Micro-organism and inoculum preparation**

239 *E. coli* SOR 201 (isolated from cheese), provided by SOREDAB Laboratory (France), was

240 stored at -80 °C in nutrient broth supplemented with 50% glycerol. The inoculum was

241 prepared by subculturing the bacterial strain in 100 mL of nutrient broth (tryptone 10 g/L,

242 meat extract 5 g/L and sodium chloride 5 g/L. pH 7.2±0.2) at 37 °C on a rotary shaker (100

243 rpm), subsequently for 8 h and 16 h.

244 **3.2. Experimental setup for the model validation at constant air temperature and**

245 **changing convective heat transfer coefficient**

246 **3.2.1. Growth measurement**

247 Growth curves were determined by the measurement of absorbance changes with a

248 spectrophotometer (Milton Roy, Spectronic 301) at 600 nm wavelength. Absorbance was

249 measured with sterile nutrient broth as a blank. Samples were filled in glass "growth flasks"

250 specially designed for the measurement of the absorbance of the content without sampling. A

251 calibration experiment was done to determine the correlation between viable counts and

252 absorbance data in nutrient broth permitting the estimation of the bacterial concentrations

253 from absorbance values. Samples were incubated at 30 °C in a shaking water bath and

254 bacteria were grown until stationary phase. The optical density was periodically measured and

255 one mL was simultaneously removed from the solution to be analyzed by the plate count

256 method. The experimental dataset was fitted with the exponential model proposed by Juarez

257 Tomas et al. (2002) to fit the calibration equation which can be written as follows:

$$LnN = a(OD)^b \qquad\qquad (16)$$

259 Where N is the bacterial concentration, OD is the corresponding optical density (600 nm)

260 measured at time t and a and b are empirical parameters.

261 Fig. 1 depicts the experimental data and the calibration curve relating OD to viable counts.

262 Estimates of parameters a and b were respectively assessed to 22.8 [22.6 .. 22.9] and 0.090

263 [0.087 .. 0.093] ($R^2 = 0.999$ and $MSE = 0.009$).

264 Francois et al. (2005) demonstrated that a temperature of 4 °C had no significant statistical

265 effect on the linear calibration curve compared to optimal conditions (T 30 °C, pH 7,4 and a_w

266 0.995) in BHI medium. Consequently, we didn't perform the calibration experiment at other

267 temperatures than 30 °C (the initial product temperature at all the experiments).

3.2.2. Simulation design

269 Five combinations of thickness of an infinite slab, convective heat transfer coefficient and

270 chilling temperature were input (Fig. 2) for the calculation of thermal parameters j and k. A

271 simulated growth curve related to each combination was then calculated from Eqs. (14) and

272 (15). An h value of 8 W/(m^2.K) corresponds to the absence of fan (particularly in unventilated

273 zones or in equipment inside which heat is transferred by natural convection) while an h value

274 of 60 W/(m^2.K) corresponds to a strong air fan (in the case of forced convection). Moreover,

275 according to Kondjoyan (2006), average heat transfer coefficient values (W/(m^2.K))

276 calculated under different air velocity (0.2 – 5.0 m s^{-1}) and free-stream turbulence intensity

277 conditions (5 – 40 %) ranged from 1.3 to 42.0 for a circular cylinder and from 2.3 to 60.0 for

278 meat products (Beef carcass, pork hindquarter and lamb carcass (loin)). Furthermore, Ben

279 Amara et al. (2004) studied the effect of various factors (air velocity, position, air-product

280 temperature difference) on the transfers during cooling with a low air velocity (< 0.2 m/s), of

281 an in-line stack of spheres and measured h values ranging from 8 to 19 W/(m^2.K) for air

282 velocity varying from 0.03 to 0.19 m s^{-1}.

283 **3.2.3. Conditions of growth for the validation of the model**

284 Corresponding to each combination of slab thickness and convective heat transfer coefficient,

285 cooling profiles and bacterial growth were simulated at the centre and at the surface of an

286 infinite slab shaped product. The product thermal diffusivity and thermal conductivity values

287 input in the calculations were assumed to be equal to those of water determined at 25 °C, i.e.

288 $1.43.10^{-7}$ m^2/s and 0.6 W/(m.K) respectively.

289 Furthermore, input μ_{opt}, T_{min} and T_{opt} values of *E. coli* SOR 201 were respectively equal to

290 2.66 h^{-1}, 3.28 °C and 42.03 °C in nutrient broth. These values were estimated from forty six

291 growth kinetics conducted at 11 constant temperatures ranging from 10 °C to 46 °C.

292 Experimental datasets were fitted and growth curve parameters (maximum growth rate (μ_{max}),

293 lag time, initial and maximum population densities) were estimated from the primary growth

294 model of Baranyi and Roberts (1994). The obtained μ_{max} values were fitted with the

295 secondary cardinal model (Rosso et al., 1995) in order to estimate the optimal growth rate and

296 the cardinal temperatures of *E. coli* SOR 201 (see Fig. A2 in the appendix).

297 In order to validate the overall mathematical model developed in the present work,

298 experiments were conducted under a changing temperature program which corresponds to the

299 simulated cooling profiles of the surface or the centre of the product. All the prepared material

300 was pre-chilled/heated to the initial temperature (30 °C). Subculture was diluted to provide an

301 inoculation level ranging from 10^6 to 10^7 CFU/mL at the starting of the test. Samples were

302 filled in glass "growth flasks" allowing the measurement of the absorbance of the content,

303 during the experiment, without sampling. Their shaking was guaranteed by a magnetic

304 shaking table. Samples were instantly incubated and periodically removed so as to measure

305 optical densities (at 600 nm) in the course of the experiment. Experiments were carried out in

306 triplicate. The chilling was monitored with a refrigerated and heating circulator (FP40-HE,

307 Julabo Labortechnik GmbH, Germany) allowing a temperature stability of ±0.01 °C.

308   **3.3. Experimental setup for the model validation at changing air temperature and**

309   **constant convective heat transfer coefficient**

310   For a further validation of the model, more complicated temperature scenarios were tested

311   assuming alternated cooling and heating stages. Moreover, an inoculation level ranging from

312   10^3 to 10^4 CFU/mL was used in order to consider more realistic bacterial concentrations

313   encountered in food industry processes.

314   Three different ambient air temperature scenarios, drawn from real refrigerated food

315   processes, were tested (cf. Table 2).

316   Corresponding to each air temperature scenario, temperature profiles and bacterial growth

317   were simulated at the centre and at the surface of an infinite slab shaped product. At all the

318   tested temperature scenarios, the initial product temperature, the product thickness and the

319   convective heat transfer coefficient were respectively equal to 15 °C, 0.12 m and 8 W/(m^2.K).

320   Input μ_{opt}, T_{min} and T_{opt} values of *E. coli* SOR 201 are mentioned above. Typical beef meat

321   thermal diffusivity and thermal conductivity values, respectively equal to $1.25.10^{-7}$ m^2/s and

322   0.42 W/(m.K), were input in the calculations.

323   Experiments were conducted under thermal programs which corresponded to the simulated

324   temperature profiles of the surface or the centre of the product. Subculture was diluted,

325   samples were filled in glass "growth flasks", instantly incubated and periodically removed so

326   as to perform the viable count measurement in the course of the experiment. Experiments

327   were carried out in duplicate. The thermal program was monitored with the refrigerated and

328   heating circulator (FP40-HE, Julabo Labortechnik GmbH, Germany). At each sampling time,

329   1-mL aliquots were aseptically removed from each "growth flask", serially diluted in tryptone

330   salt broth and plated on nutrient agar (15 g/L) with a double layer. Petri dishes were incubated

331   at 37 °C for 24 h and colonies were counted.

332   **3.4. Validation and assessment of the quality of the overall model**

333   Model accuracy was assessed by the estimation of confidence bands of predictions by using

334   the bootstrap percentile method (Efron and Tibshirani, 1993). Forty six growth kinetics were

335   performed in nutrient broth at 11 constant temperatures ranging from 10 °C to 46 °C (data not

336   shown). Bootstrap of each kinetic was made in order to take the experimental errors of

337   kinetics into account. The appropriate residuals of each kinetic were drawn with replacement.

338   Twenty five thousands bootstrap set of primary parameters were obtained. Each set of

339   bootstrapped μ_{max} values were used to fit the secondary model. Then bootstrapped values of

340   parameters T_{min}, T_{opt} and μ_{opt} were used to predict the bacterial growth with the overall model.

341   Secondary observed residuals were drawn with replacement and added to the μ predicted

342   value. Primary residuals were added to the predicted kinetics to consider the experimental

343   error of cell number estimation. Twenty five thousands bootstrapped growth kinetics were

344   obtained for each validation experiment and sorted in ascending order at each calculation

345   time. The quartiles 2.5% and 97.5% of the sorted bootstrapped kinetics were taken to give the

346   inferior and superior limits. These points were linked to give an approximation of the 95

347   percent confidence bands of the predicted growth kinetics. To validate the assumptions made

348   and the model, less than 5% of the points must fall outside the confidence bands.

349   With regard to the assessment of the quality of the overall model predictions various

350   statistical criteria were calculated at all the tested conditions of validation experiments.

351   Correlation coefficients (R) between observations and predictions were calculated using the

352   'corrcoef' function of MATLAB 6.5. The correlation coefficient is related to the covariance

353   *cov* by:

354
$$R(i, j) = \frac{\text{cov}(i, j)}{\sqrt{\text{cov}(i,i)\text{cov}(j, j)}} \qquad (17)$$

355   where i is the observations index and j is the variables index.

356 Bias factor B_f (Eq. (18)) and Accuracy factor A_f (Eq. (19)) were calculated as proposed by

357 Jeyamkondan et al. (2001). These factors were initially introduced by Ross (1996) but here,

358 the predicted values are normalized.

359 $$B_f = 10^{\sum \log(P/O)/n} \qquad (18)$$

360 $$A_f = 10^{\sum |\log(P/O)|/n} \qquad (19)$$

361 where O and P are observed and predicted microbial populations in $\log_{10}$ CFU/mL and n is

362 the number of observations. The bias factor indicates the relative average deviation of

363 predicted and observed bacterial growth. However it has to be kept in mind that this deviation

364 does not directly concern the size of the population, but its logarithmic transformation which

365 reduces the effect of outliers.

366 A bias factor of 1 indicates perfect agreement between observed and predicted values.

367 However, $B_f > 1$ or < 1 indicates that the model predicts N upper than or lower than observed

368 values. For example, $B_f = 1.1$ means that predictions are on average upper than observed

369 values by 10%. The accuracy factor gives indication of the spread of the results about the

370 predicted value. An accuracy factor of 1 represents perfect agreement between observed and

371 predicted values. This parameter quantifies the difference between observed and predicted

372 values. For example, $A_f = 1.25$ indicates that the average deviation of the predicted values

373 from the observed values is 25%. It has to be kept in mind that this deviation does not directly

374 concern the size of the population, but its logarithmic transformation.

375 **4. Results**

376 **4.1. Model validation at constant air temperature and changing convective heat transfer**

377 **coefficient**

378 **4.1.1. Growth simulation**

379 Thermal programs tested at the validation stage were utilized at five different combinations of

380 product thickness (E), convective heat transfer coefficient (h) and refrigeration temperature

381   (T_∞) (Fig. 2).

382   The obtained cooling profiles and growth predictions are presented in Fig. 3. As a rule,

383   bacterial growth kinetics were faster at the product centre than at its surface. In cases of

384   lowest thickness, simulated computing profiles (1c and 2c) were practically identical leading

385   to the same bacterial growth predictions (1g and 2g) at the centre and at the surface of the

386   product. In fact, in these two experiments the product thickness was sufficiently low to

387   prevent a clear observation of an internal temperature gradient and the internal heat resistance

388   may had been neglected. In contrast, the difference between simulated theoretical temperature

389   kinetics at the centre and the surface of the product were more marked in the cases of the

390   highest thickness leading to an important thermal gradient within the product (3c and 4c). For

391   that matter, the most important differences between internal and surface growth kinetics were

392   obtained in these two cases (3g and 4g), particularly in the case of low heat transfer

393   coefficient.

394   On the other hand, additional simulated growth curves at constant temperatures equal to T_∞

395   were presented in Fig. 3. The aim of these further experiments was to compare the bacterial

396   growth that really occurs when temperature dynamic changes at the centre and at the surface

397   of the cooled product are considered, with the growth that would occur if external and internal

398   resistances were neglected.

399   **4.1.2. Validation results**

400   Each validation experiment regarding each (T_∞, h, E) combination (Fig. 2) was conducted

401   under two different refrigeration programs which corresponded to the simulated cooling of the

402   surface and the centre of the infinite slab-shaped product yielding a total of eight validation

403   tests. These tests lasted 24 hours with an initial temperature T_0 of 30 °C. In order to validate

404   the overall mathematical model, Fig. 4 depicts predicted and observed *E. coli* SOR 201

405   growth during the simulated cooling at the centre or the surface of the product for the five

406 cases presented in Fig. 2. A fair agreement between predicted and observed growth can be

407 noted, and the observed growth data of *E. coli* SOR 201 were found to be adequately

408 predicted by the overall mathematical model. For each predicted growth kinetic, 95 percent

409 confidence bands calculated with bootstrap method are also presented in Fig. 4. All the

410 experimental data fell inside the confidence bands showing that the overall model was

411 successfully validated at the tested conditions.

412 On the other hand, the quality of the overall model prediction was assessed by the calculation

413 of correlation coefficient, B_f and A_f (see Table 3). The correlation coefficients were higher

414 than 0.975 showing that the bacterial growth was satisfactorily predicted by the overall

415 model. At all the instances, bias factors ranged from 0.98 to 1.00 indicating that ~~on average,~~

416 ~~the observed growth was at the most 2% higher than the predicted growth and that~~ the overall

417 predictions agreed well with observed data with a slight under-prediction tendency by the

418 model. ~~In all the tested conditions, the percentage of predicted values which were different~~

419 ~~(either above or below) than the observed values was at the most equal to 5% as can be noted~~

420 ~~from Af values ranging from 1.01 to 1.05.~~

421 Agreement between model predictions and experimental validation results was also assessed

422 by plotting predicted bacterial growth versus observed bacterial growth (Fig. 5). A perfect

423 agreement between predicted and measured growth was observed for 30.80% of experimental

424 data. A percentage of 25.36% of the observed–predicted values' pairs were laying under the

425 line of equivalence while 43.84% were laying above the line of equivalence.

426 **4.2. Model validation at changing air temperature and constant convective heat transfer**

427 **coefficient**

428 **4.2.1. Growth simulation**

429 Fig. 6 illustrates the simulated thermal profiles and bacterial growth kinetics according to the

430 conditions presented in Table 2 and §3.3. Thermal and bacterial growth simulation results

431   showed important differences of temperature profiles and growth between the product centre,

432   the product surface and the ambient air. During heating, the highest bacterial growth was

433   observed when simulations were carried out at air temperature, followed by the product's

434   surface and then by the product's centre. Conversely, an opposite trend was observed during

435   cooling. From a safety point of view, neglecting heat transfer phenomena that occur inside the

436   product and between the ambient air and the product is more dangerous at cooling stages than

437   at heating stages. Nevertheless this hazard depends on the temperature and duration history of

438   the cooling/heating stages. Consequently it's very important to take into account the actual

439   temperature of the product surface or centre rather than the ambient air temperature for a

440   reliable bacterial growth prediction.

441   **4.2.2. Validation results**

442   Validation results regarding the three tested ambient scenarios are presented in figures 7 and

443   8. The observed growth data of *E. coli* SOR 201 were found to be adequately predicted by the

444   overall mathematical model. On the other hand, less than 5% of the experimental data fell

445   outside the 95 percent confidence bands showing that the overall model was successfully

446   validated at the tested conditions. Table 4 presents the statistical criteria related to the data of

447   validation at changing air temperature and shows correlation coefficients higher than 0.944 at

448   all the tested conditions. Bias factors obtained at all the assays were higher than 1 showing a

449   slight over-prediction tendency by the model. A_f values (lower than 1.13 at all the instances)

450   indicate that the overall predictions agreed well with observed data. Fig. 8 shows predicted

451   bacterial growth versus observed bacterial growth and confirms that the overall model was

452   successfully validated, with a slight over-prediction tendency, for the tested dynamic

453   refrigeration cycles.

454   **5. Discussion**

20

455   Traditionally, when simulating a bacterial growth during a product cooling or heating,

456   predictive microbiology took only the ambient air temperature into account, ignoring delays

457   and temperature gradients due to external and internal thermal resistances linked to the effects

458   of the medium thickness and of the convective heat transfer coefficient on the rate of heat

459   transfer. All the studies cited in Table 1 have evaluated the prediction of bacterial growth

460   under dynamic temperature conditions taking into account only the temperature of the

461   cooling/heating medium. Assuming that the bacterial growth directly occurs at the

462   temperature of air is not valid. In fact, the local temperature at any given position in the

463   product depends upon both T_∞ and h. In the present study, predictive microbiology was

464   combined with heat transfer phenomena in order to develop an overall mathematical model

465   describing the effect of the ambient temperature and the convective heat transfer coefficient

466   on bacterial growth. The proposed method in this work is different than those in previous

467   studies which combined predictive microbiology and heat transfer (Alavi et al., 2001;

468   Amezquita et al., 2005; Bellara et al., 2000; Corradini et al., 2006). An experimental method

469   was implemented in order to validate the model results. Thermal profiles were firstly

470   simulated at the centre and at the surface of the infinite slab shaped product. Then,

471   experiments were conducted under a changing temperature program corresponding to the

472   simulated temperature kinetics. The validation of the overall model was performed by the

473   comparison of the measured bacterial growths with model predictions at constant ambient air

474   temperature and changing convective heat transfer coefficient and product thickness (five

475   different combinations of product thickness, convective heat transfer coefficient and cooling

476   air temperature were tested), then at changing ambient air temperature and fixed convective

477   heat transfer coefficient and product thickness (three different ambient air scenarios assuming

478   alternated cooling and heating stages, drawn from real refrigerated food processes, were

479   tested).

480   As expected, the results of the computer simulation related to single cooling stage

481   experiments showed that the bacterial growth kinetics were faster at the product centre than at

482   its surface. Moreover, the importance of the impact of the convective heat transfer coefficient

483   and of the product thickness on the bacterial growth during the cooling of an infinite slab

484   shaped product by pulsed air was pointed out. As an example, at the product half thickness,

485   the level of bacterial growth accomplished after 5 hours of cooling with $h = 8$ W/(m^2.K) (case

486   3) was the same after 16.5 hours with $h = 60$ W/(m^2.K) (case 4). For these cases the product

487   thickness was the same and the cooling air temperature was in case 3 4°C lower than in case

488   4. Similarly, at product half thickness, the cooling time needed to reach a same bacterial

489   growth with low or high product thickness (1 cm in case 2 and 6 cm in case 4) was estimated

490   to 17.5 hours and 8 hours, respectively, for the same convection level (60 W/(m^2.K)). The

491   slowest simulated bacterial growth was observed with intermediate product thickness and

492   convective heat transfer coefficient (case 5). Moreover, it obviously appears that the validity

493   of the assumption of an instantaneously thermal equilibrium between the product and the

494   cooling medium with regard to bacterial growth is depending on the level of convection. In

495   fact, predicted growth kinetics at the surface of the product were close to those predicted at T_∞

496   for high heat transfer coefficients (h) equal to 60 W/(m^2.K), which corresponds to a strong air

497   fan (Fig. 3: 2g and 4g). At this instance, neglecting the external heat resistance may be

498   accepted particularly for low product thickness (1 cm) where there's no internal heat

499   resistance too. Oppositely, for low heat transfer coefficients (h) equal to 8 W/(m^2.K), which

500   corresponds to the absence of fan, (Fig. 3: 1g and 3g) important dissimilarities between

501   predicted growth kinetics at the surface of the product and at T_∞ may be observed. Indeed,

502   assuming no external heat transfer resistance is not valid especially for high product thickness

503   of 6 cm (Fig. 3: 3g) where the bacterial growth that occurs when the product is cooled from T_0

504   to T_∞ was clearly higher than that at an immediately reached temperature T_∞. In this case, a

505   difference of 1.35 $\log_{10}$(CFU/mL) between the bacterial populations at the product surface

506   and at T_∞ was reached after 24 hours of growth. Besides, using the bootstrap percentile

507   method for the estimation of confidence bands of predictions, the model was successfully

508   validated at all the tested conditions.

509   Concerning the results related to alternated cooling and heating stage experiments, the model

510   was successfully validated at more complicated ambient air scenarios and lower inoculation

511   levels by plate count measurement method. These results showed that, in predictive

512   microbiology, assuming an instantaneously thermal equilibrium between the product and the

513   ambient medium is not valid and may have large consequences on risk assessment of

514   refrigerated food processes (see Fig. 9).

515   To assess the quality of the overall model, predicted bacterial growth was compared to

516   observed growth according to several statistical criteria related to the data of validation. Our

517   results pointed out a good agreement between predicted and observed growth.

518   On the other hand, in the overall model, as a primary bacterial model, a simple exponential

519   growth without lag time was assumed. In other words, it is supposed that the bacterial growth

520   occurred without delay when the product temperature was continuously changing. Our

521   assumption is in agreement with several previous studies. Although the fact that organisms

522   need to adapt to the new temperature, so that they go through a lag phase caused by the stress

523   of the temperature shift, was largely noticed in literature (Amezquita et al., 2005; Baranyi et

524   al., 1995; Koutsoumanis, 2001; Zwietering et al., 1994), the lag phase duration was rarely

525   considered in predictive models. In accordance with our work, no further delay occurring after

526   temperature shifts, once a cell population is growing exponentially, was frequently assumed

527   (Baranyi et al., 1995; Bovill et al., 2000; Koutsoumanis et al., 2006). Although, Swinnen et al.

528   (2005) demonstrated that temperature shifts crossing a lag/no lag transition zone (positioned

529   more or less between 22.78 and 23.86 °C for *E. coli* K12 MG1655) will cause an intermediate

530   lag phase, we consider that neglecting contingent intermediate lag phase by our model may be

531   a valid approach. In fact, simulated thermal profiles at product surface or centre due to heat

532   transfer phenomena (see Fig. 3 and Fig. 6) progressively changed with time and cannot be

533   regarded as instantaneous temperature shifts with given amplitude which may generate

534   intermediate lag phases.

535   Paradoxically, the complexity of foods' shapes and the lack of knowledge about their physical

536   properties dictate the utilization of simple model. We took as an example the case of infinite

537   slab, but the model can be generalised to complex shapes. A classical and relevant approach is

538   of course, the implementation of numerical modelling. Another approach is related to the

539   well-known Ball method (Ball, 1923) with its two empirical parameters, for heat treatment

540   processes calculations. Because foodstuffs shapes are complex and because their thermal

541   properties are often unknown, it can be relevant to implement a simple model including only

542   two parameters (j and k of Eq. (1)) which can be easily empirically estimated from a simple

543   temperature registration and a simple linear regression of the reduced temperature (which is

544   linearised from a logarithmic transformation). Note that errors which can be generated by

545   "simplistic" heat transfer models are minor compared to errors which are linked to the

546   "biological background". Moreover, the overall model can be used for any bacterial strain

547   having known growth parameters T_{min}, T_{opt} and μ_{opt}. Accordingly, the proposed model can be

548   used for designing safe cooling or heating processes and may be considered as a very useful

549   tool for risk assessment regarding food safety and process optimisation.

6. Appendix

551   Equation of the the infinite series given by Carslaw and Jaeger (1986):

552
$$\frac{T_\infty - T}{T_\infty - T_0} = \sum_1^\infty \frac{2\sin\varphi_n}{\varphi_n + \sin\varphi_n \cos\varphi_n} \cos\left(\varphi_n \frac{x}{x_{\max}}\right) \exp\left(-\varphi_n^2 Fo\right)$$ (20)

553   with x_{max} is half-thickness for an infinite slab and φ_n are the roots of the equation $\cot\varphi = \dfrac{\varphi}{Bi}$.
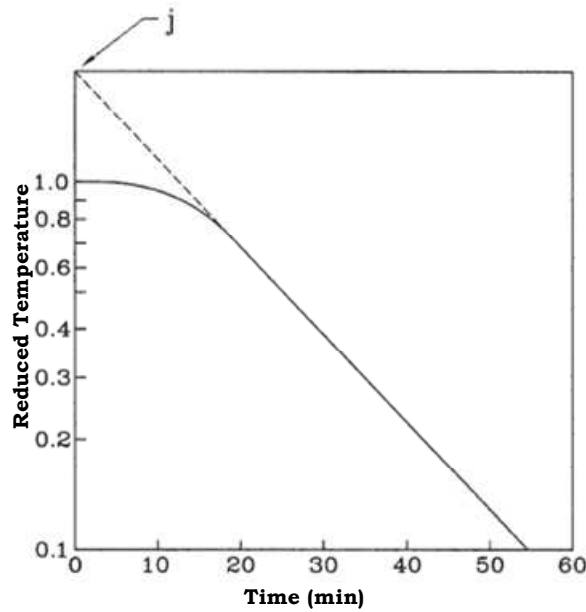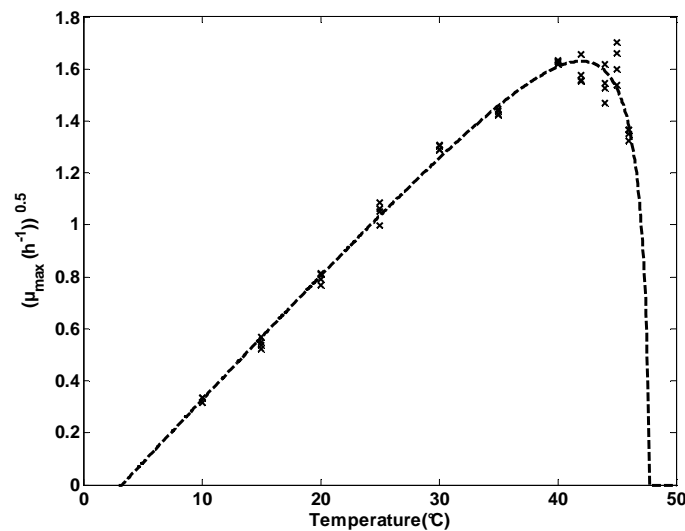

554

555   Fig. A1. Typical cooling curve (Becker and Fricke, 2004)

556

557

558   Fig. A2. Fit of the cardinal model on $\mu_{\max}$ values measured in nutrient broth ($\times$). The dashed

559   line denotes the fitted model on the experimental data.

25

560 **References**

561

562   Alavi, S.H., Puri, V.M., Mohtar, R.H. 2001. A model for predicting the growth of

563 *Listeria monocytogenes* in packaged whole milk. Journal of Food Process Engineering 24,

564 231–251.

565   Amezquita, A., Weller, C.L., Wang, L., Thippareddi, H., Burson, D.E. 2005.

566 Development of an integrated model for heat transfer and dynamic growth of *Clostridium*

567 *perfringens* during the cooling of cooked boneless ham. International Journal of Food

568 Microbiology 101, 123-144.

569   Armitage, N.H. 1997. Use of predictive microbiology in meat hygiene regulatory

570 activity. International Journal of Food Microbiology 36, 103-109.

571   Ball, C. 1923. Thermal process times for canned foods. Bulletin 7-1, 37 (National

572 Research Council, Washington, DC).

573   Baranyi, J., Roberts, T.A. 1994. A dynamic approach to predicting bacterial growth in

574 food. International Journal of Food Microbiology 23, 277-294.

575   Baranyi, J., Robinson, T.P., Kaloti, A., Mackey, B.M. 1995. Predicting growth of

576 *Brochothrix thermosphacta* at changing temperature. International Journal of Food

577 Microbiology 27, 61-75.

578   Becker, B.R., Fricke, B.A. 2004. Heat transfer coefficients for forced-air cooling and

579 freezing of selected foods. International Journal of Refrigeration 27, 540-551.

580   Bellara, S.R., McFarlane, C.M., Thomas, C.R., Fryer, P.J. 2000. The growth of

581 *Escherichia coli* in a food simulant during conduction cooling: combining engineering and

582 microbiological modelling. Chemical Engineering Science 55, 6085-6095.

583   Ben Amara, S., Laguerre, O., Flick, D. 2004. Experimental study of convective heat

584   transfer during cooling with low air velocity in a stack of objects. International Journal of

585   Thermal Sciences 43, 1213-1221.

586   Bimbenet, J.J., Duquenoy, A., Trystram, G. 2002. Génie des procédés alimentaires. Des

587   bases aux applications. Dunod ed., Paris, France.

588   Bovill, R., Bew, J., Cook, N., D'Agostino, M., Wilkinson, N., Baranyi, J. 2000.

589   Predictions of growth for *Listeria monocytogenes* and *Salmonella* during fluctuating

590   temperature. International Journal of Food Microbiology 59, 157–165.

591   Bovill, R.A., Bew, J., Baranyi, J. 2001. Measurements and predictions of growth for

592   *Listeria monocytogenes* and *Salmonella* during fluctuating temperature II. Rapidly changing

593   temperatures. International Journal of Food Microbiology 67, 131–137.

594   Caro-Corrales, J., Cronin, K., Abodayeh, K., Gutiérrez-López, G., Ordorica-Falomir, C.

595   2002. Analysis of random variability in biscuit cooling. Journal of Food Engineering 54, 147-

596   156.

597   Carslaw, H.S., Jaeger, J.C. 1986. Conduction of Heat in Solids. 2nd ed. Oxford

598   University Press.

599   Corradini, M.G., Amézquita, A., Normand, M.D., Peleg, M. 2006. Modeling and

600   predicting non-isothermal microbial growth using general purpose software. International

601   Journal of Food Microbiology 106, 223–228.

602   Dalgaard, P. 1995. Modelling of microbial activity and prediction of shelf life for

603   packed fresh fish. International Journal of Food Microbiology 26, 305-317.

604   de Jong, A.E.I., Beumer, R.R., Zwietering, M.H. 2005. Modeling growth of *Clostridium*

605   *perfringens* in pea soup during cooling. Risk Analysis: An International Journal 25, 61-73.

606   Dincer, I. 1996. An exact solution on the estimation of heat-transfer rates during deep-

607   freezing of slab products. Journal of Food Engineering 30, 417-423.

608   Efron, B., Tibshirani, R.J. 1993. Confidence intervals based on bootstrap percentiles. In:

609 An introduction to the Bootstrap. Chapman and Hall, New York, pp. 168-177.

610   Erdogdu, F. 2005. Mathematical approaches for use of analytical solutions in

611 experimental determination of heat and mass transfer parameters. Journal of Food

612 Engineering 68, 233-238.

613   Francois, K., Devlieghere, F., Standaert, A.R., Geeraerd, A.H., Cools, I., Van Impe,

614 J.F., Debevere, J. 2005. Environmental factors influencing the relationship between optical

615 density and cell count for *Listeria monocytogenes*. Journal of Applied Microbiology 99, 1503-

616 1515.

617   Fujikawa, H., Kai, A., Morozumi, S. 2004. A new logistic model for *Escherichia coli*

618 growth at constant and dynamic temperatures. Food Microbiology 21, 501–509.

619   Gibson, A.M., Bratchell, N., Roberts, T.A. 1987. The effect of sodium chloride and

620 temperature on the rate and extent of growth of *Clostridium botulinum* type A in pasteurized

621 pork slurry. Journal of Applied Bacteriology 62, 479-490.

622   Gill, C.O., Harrison, J.C.L. 1985. Evaluation of the hygienic efficiency of offal cooling

623 procedures. Food Microbiology 2, 63-69.

624   Gumudavelli, V., Subbiah, J., Thippareddi, H., Velugoti, P.R., Froning, G. 2007.

625 Dynamic predictive model for growth of *Salmonella Enteritidis* in egg yolk. Journal of Food

626 Science 72, M254-M262.

627   Huang, L. 2003. Dynamic computer simulation of *Clostridium perfringens* growth in

628 cooked ground beef. International Journal of Food Microbiology 87, 217–227.

629   Jeyamkondan, S., Jayas, D.S., Holley, R.A. 2001. Microbial growth modelling with

630 artificial neural networks. International Journal of Food Microbiology 64, 343-354.

631   Juarez Tomas, M.S., Bru, E., Wiese, B., de Ruiz Holgado, A.A.P., Nader-Macias, M.E.

632 2002. Influence of pH, temperature and culture media on the growth and bacteriocin

633 production by vaginal *Lactobacillus salivarius* CRL 1328. Journal of Applied Microbiology

634 93, 714-724.

635 Juneja, V.K., Marks, H., Thippareddi, H. 2008. Predictive model for growth of

636 *Clostridium perfringens* during cooling of cooked uncured beef. Food Microbiology 25, 42-

637 55.

638 Kondjoyan, A. 2006. A review on surface heat and mass transfer coefficients during air

639 chilling and storage of food products. International Journal of Refrigeration 29, 863-875.

640 Koseki, S., Isobe, S. 2005. Prediction of pathogen growth on iceberg lettuce under real

641 temperature history during distribution from farm to table. International Journal of Food

642 Microbiology 104, 239–248.

643 Koutsoumanis, K. 2001. Predictive modeling of the shelf life of fish under

644 nonisothermal conditions. Applied and Environmental Microbiology 67, 1821–1829.

645 Koutsoumanis, K., Stamatiou, A., Skandamis, P., Nychas, G.J.E. 2006. Development of

646 a microbial model for the combined effect of temperature and pH on spoilage of ground meat,

647 and validation of the model under dynamic temperature conditions. Applied and

648 Environmental Microbiology 72, 124-134.

649 Lebert, I., Lebert, A. 2006. Quantitative prediction of microbial behaviour during food

650 processing using an integrated modelling approach: a review. International Journal of

651 Refrigeration 29, 968-984.

652 Mafart, P. 1997. Génie industriel Alimentaire. Tome 1: Les procédés physiques de

653 conservation. Lavoisier Techniques & Documentations ed., Paris, France.

654 Mafart, P. 2005. Food engineering and predictive microbiology: on the necessity to

655 combine biological and physical kinetics. International Journal of Food Microbiology 100,

656 239-251.

657   McMeekin, T.A., Brown, J., Krist, K., Miles, D., Neumeyer, K., Nichols, D.S., Olley, J.,

658   Presser, K., Ratkowsky, D.A., Ross, T., Salter, M., Soontranon, S. 1997. Quantitative

659   Microbiology: A Basis for Food Safety. Emerging Infectious Diseases 3, 541-550.

660   McMeekin, T.A., Olley, J.N., Ross, T., Ratkowsky, D.A. 1993. Predictive

661   Microbiology: theory and application Research Studies Press, Taunton, Somerset, England.

662   Ratkowsky, D.A., Olley, J., McMeekin, T.A., Ball, A. 1982. Relationship between

663   temperature and growth rate of bacterial cultures. Journal of Bacteriology 149, 1-5.

664   Ross, T. 1996. Indices for performance evaluation of predictive models in food

665   microbiology. Journal of Applied Bacteriology 81, 501-508.

666   Rosso, L., Lobry, J.R., Bajard, S., Flandrois, J.P. 1995. Convenient model to describe

667   the combined effects of temperature and pH on microbial growth. Applied and Environmental

668   Microbiology Vol. 61, p. 610–616.

669   Swinnen, I.A.M., Bernaerts, K., Gysemans, K., Van Impe, J.F. 2005. Quantifying

670   microbial lag phenomena due to a sudden rise in temperature: a systematic macroscopic

671   study. International Journal of Food Microbiology 100, 85.

672   U.S.D.A. 1999. Performance standards for the production of certain meat and poultry

673   products. Final rule. Federal Register 64, 732-749.

674   Zwietering, M.H., De Koos, J.T., Hasenack, B.E., De Wit, J.C., Van't Riet, K. 1991.

675   Modeling of bacterial growth as a function of temperature. Applied and Environmental

676   Microbiology 57, 1094-1101.

677   Zwietering, M.H., De Wit, J.C., Cuppers, H.G.A.M., Van't Riet, K. 1994. Modeling of

678   bacterial growth with shifts in temperature. Applied and Environmental Microbiology 60,

679   204-213.

680   Zwietering, M.H., Hasting, A.P.M. 1997. Modelling the hygienic processing of foods -

681   Influence of individual process stages. Food and Bioproducts Processing 75, 168-173.

682   Zwietering, M.H., Wijitzes, T., de Wit, J.C., Van't Riet, K. 1992. A decision support

683   system for prediction of the microbial spoilage in foods. Journal of Food Protection 55, 973-

684   979.

685

686

687 **Figure captions**

688

689 Fig. 1.

690

691 Calibration curve between viable counts and absorbance data depicted with solid line.

692 Experimental data measured at 30°C in nutrient broth are marked with (o).

693

694 Fig. 2.

695

696 Experimental design implemented for the validation of the overall model at different

697 combinations (mentioned with numbers from 1 to 5) of product thickness (E), convective heat

698 transfer coefficient (h) and refrigeration temperature (T_∞).

699

700 Fig. 3.

701

702 Cooling scenarios (from 1c to 5c) and bacterial growth curves (from 1g to 5g) obtained from

703 simulation of the overall model at the five cases of the experimental design. Symbols in

704 predicted cooling profiles: temperature of product centre (line —) and temperature of product

705 surface (line — · —). Symbols in predicted growth curves: bacterial growth at product centre

706 (line —), bacterial growth at product surface (line — · —) and bacterial growth that occurs at

707 T_∞ (line **.....**).

708

709 Fig. 4.

710

711 Comparison of predicted and observed *Escherichia coli* SOR 201 growth during cooling. *a*:

712 case1 at the centre or the surface of the product. *b*: case2 at the centre or the surface of the

713 product. *c*: case3 at the product centre. *d*: case3 at the product surface. *e*: case4 at the product

714 centre. *f*: case4 at the product surface. *g*: case5 at the product centre. *h*: case5 at the product

715 surface. Symbols in experimental data: o, □, Δ. Predicted growth curves estimated by the

716 overall model are presented with (line —). 95 percent confidence bands obtained with

717 bootstrap method are presented with (line — —).

718

719

720   Fig. 5.

721

722   Predicted bacterial growth from the overall model versus observed bacterial growth obtained

723   with constant air temperature. Symbols: □ (case 1), o (case 2). Symbols related to product

724   surface experiments: * (case 3), Δ (case 4), ◊ (case 5). Symbols related to product centre

725   experiments: • (case 3), + (case 4), x (case 5). The line of equivalence between predicted and

726   observed growth is marked with (line ─).

727

728   Fig. 6.

729

730   Thermal profiles (from 1c to 3c) and bacterial growth curves (from 1g to 3g) obtained by

731   simulation of the overall model at the three ambient air scenarios. Symbols in predicted

732   cooling profiles: temperature of product centre (line ─) and temperature of product surface

733   (line — · —). Symbols in predicted growth curves: bacterial growth at product centre (line

734   ─), bacterial growth at product surface (line — · —) and bacterial growth that occurs at T_∞

735   (line **.....**).

736

737   Fig. 7.

738

739   Comparison of predicted and observed *Escherichia coli* SOR 201 growth during thermal

740   processing at changing air temperature. *a*, *c* and *e* depict the model validation results at the

741   product centre according to cycle N°1, cycle N°2 and cycle N°3, respectively. *b*, *d* and *f*

742   depict the model validation results at the product surface according to cycle N°1, cycle N°2

743   and cycle N°3, respectively. Symbols in experimental data: o, □. Predicted growth curves

744   estimated by the overall model are presented with (line ─). 95 percent confidence bands

745   obtained with bootstrap method are presented with (line ─ ─).

746

747   Fig. 8.

748   Predicted bacterial growth from the overall model versus observed bacterial growth obtained

749   with changing air temperature. Symbols related to product surface experiments: □ (Cycle

750   N°1), * (Cycle N°2), Δ (Cycle N°3). Symbols related to product centre experiments: o (Cycle

751   N°1), • (Cycle N°2), + (Cycle N°3). The line of equivalence between predicted and observed

752   growth is marked with (line ─).

753   Fig. 9.

754   Comparison of the bacterial growth prediction at ambient temperature according to cycle N°1

755   with the model validation results at product's centre (*a*) and at product's surface (*b*). Symbols

756   in experimental data: o, □. Symbols in predicted growth curves: bacterial growth at product's

757   surface or centre (line ─), bacterial growth that occurs at T_∞ (line **.....**). 95 percent confidence

758   band of predictions at T_∞ obtained with bootstrap method is presented with (line ─ ─).

759

760

761

762
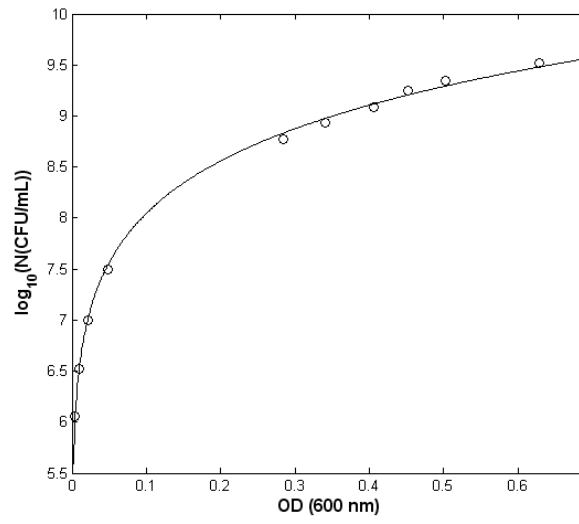
763 Fig. 1.
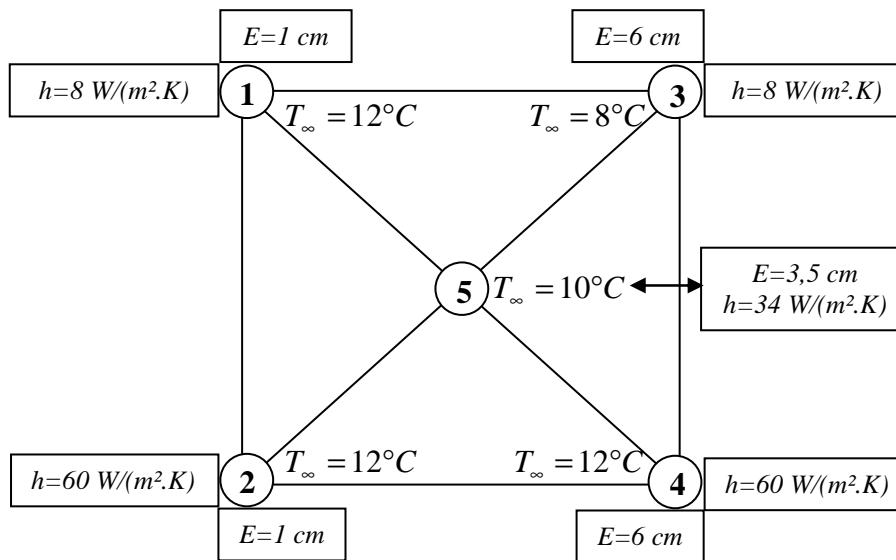
767   Fig. 2.

768
769
770
771
772
773
774
775
776
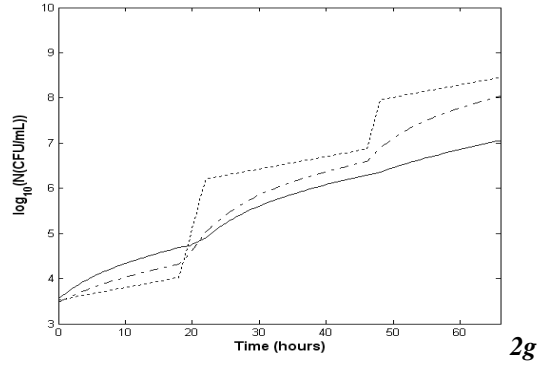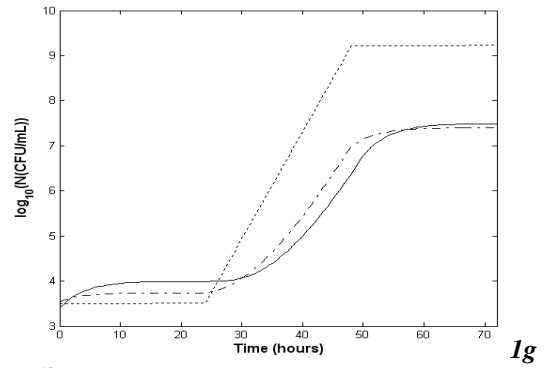777
778
779
780
781
782

783   Fig. 3.

784
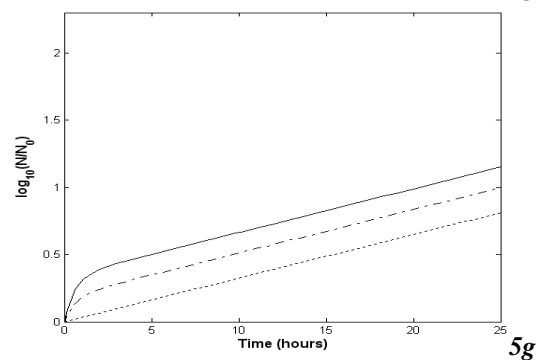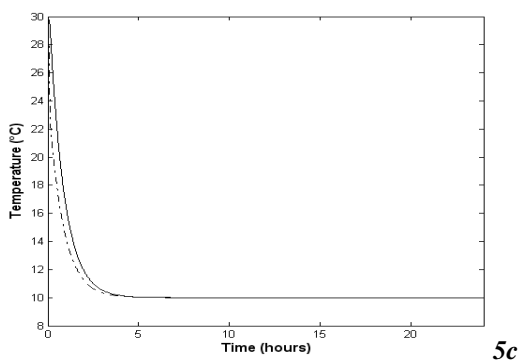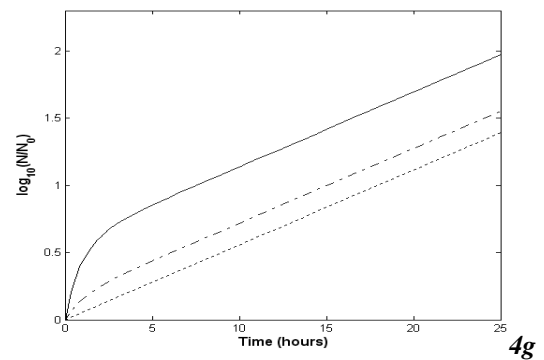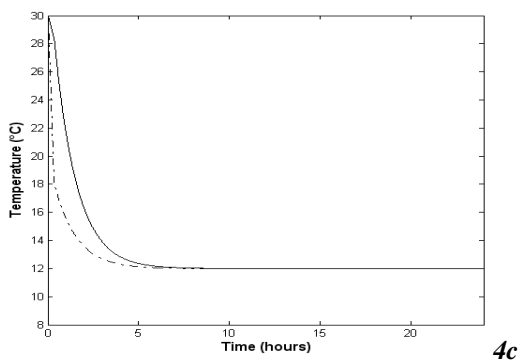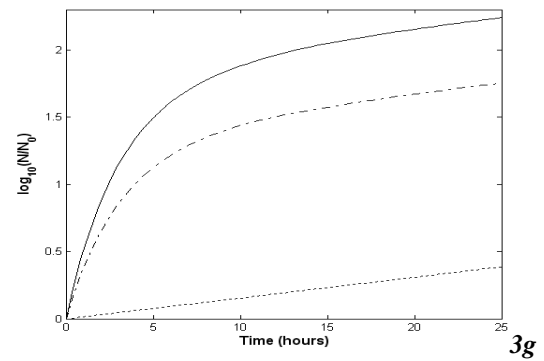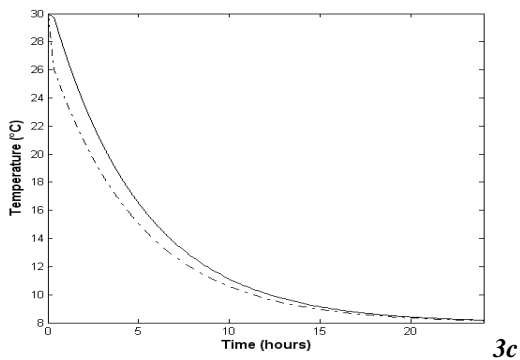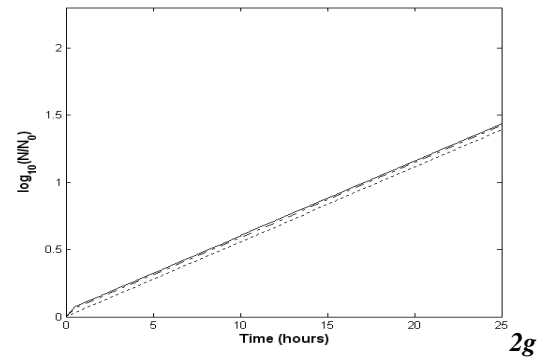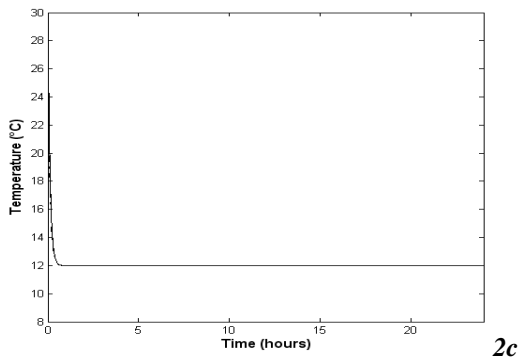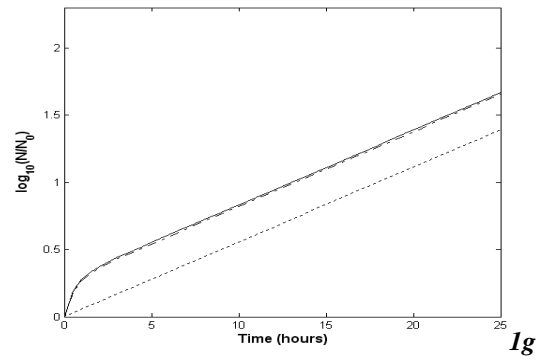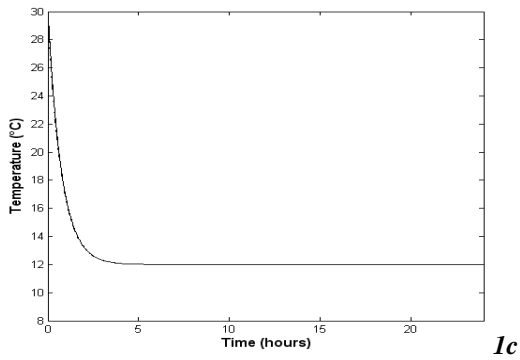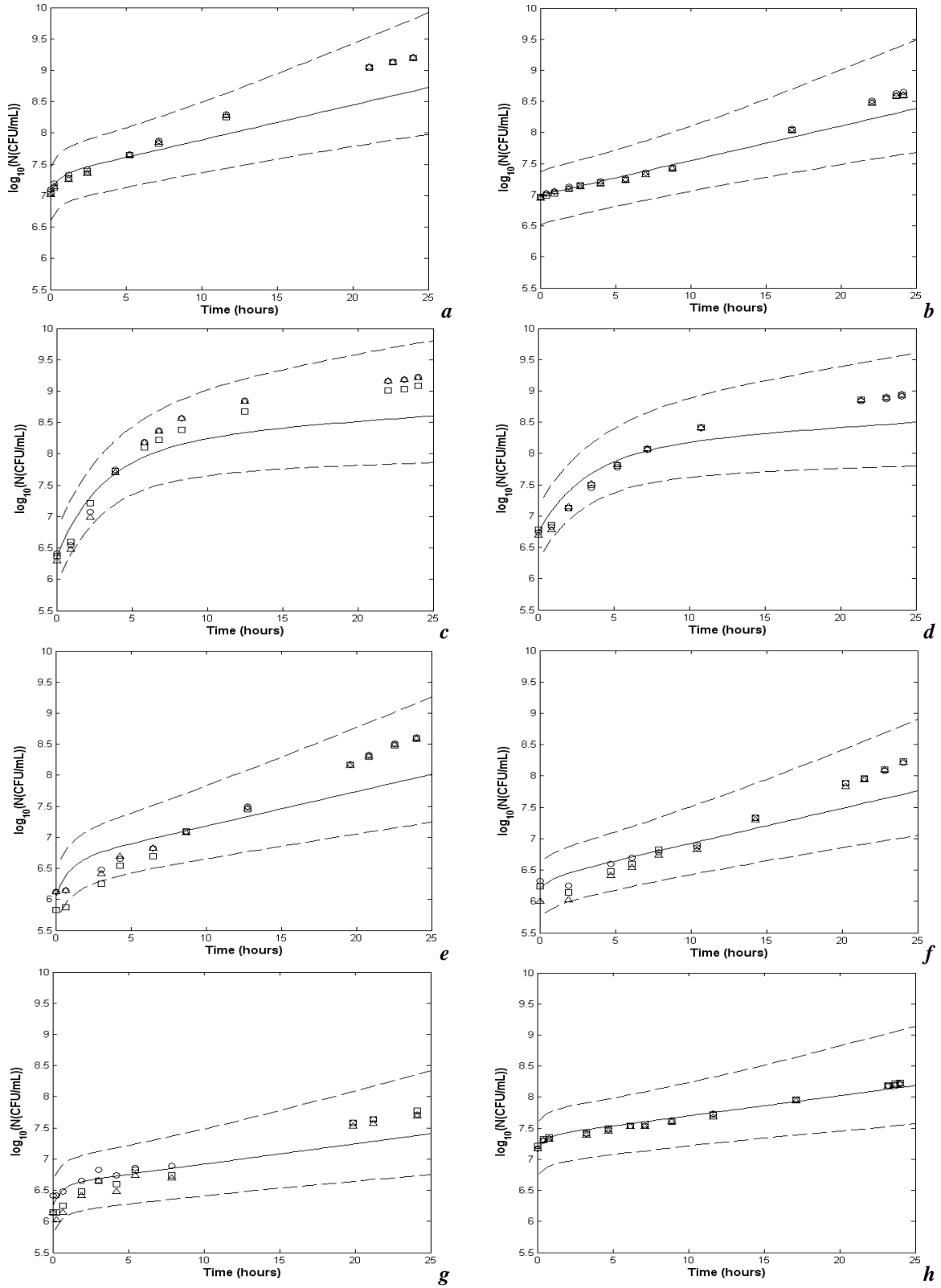
785   Fig. 4.

786

787

788
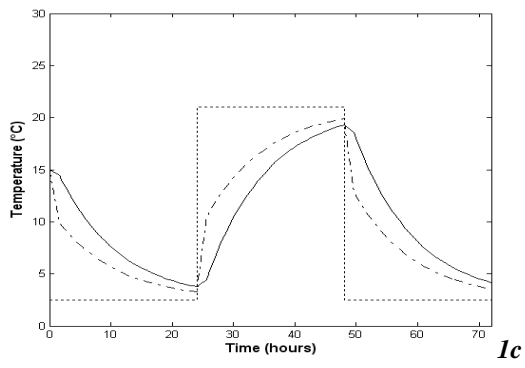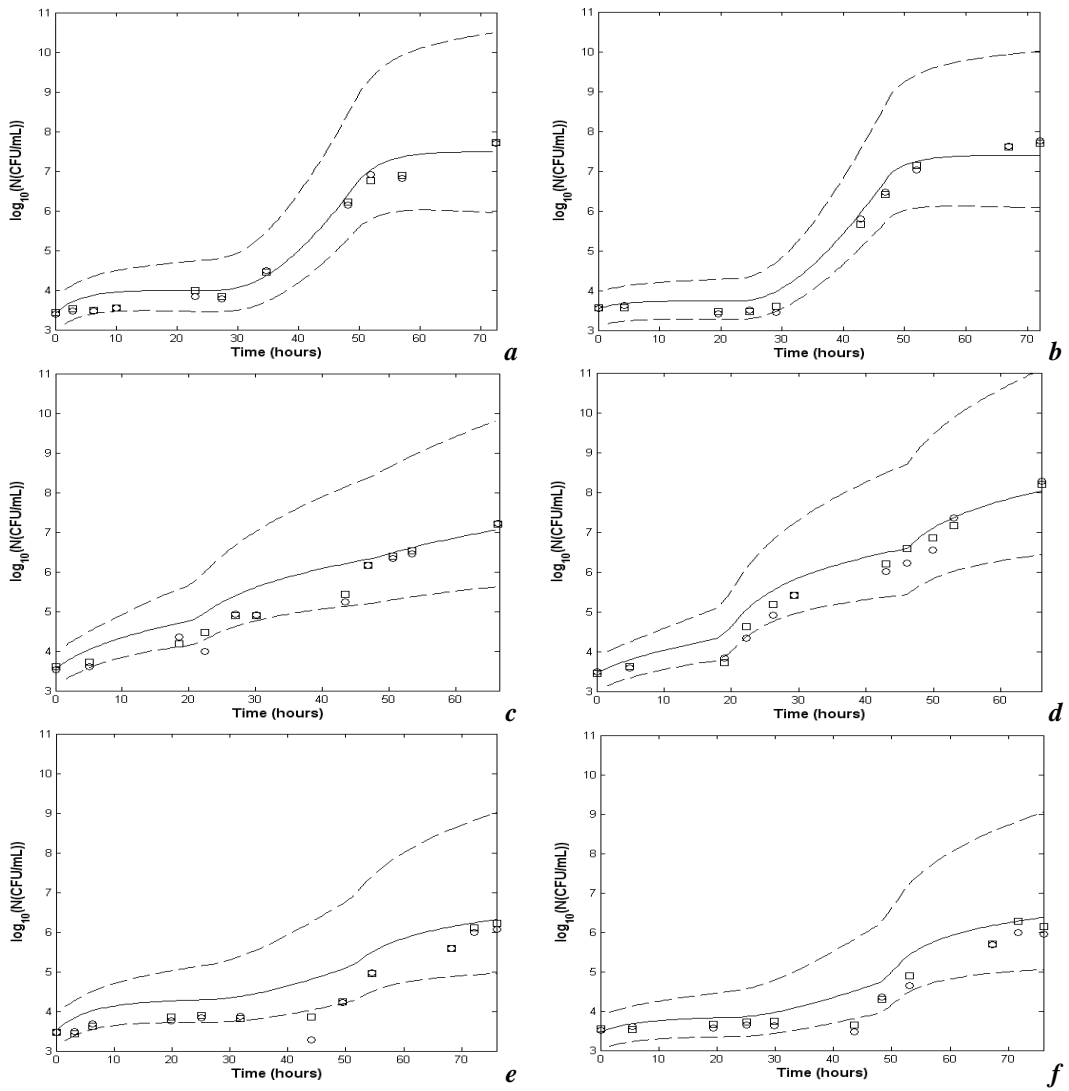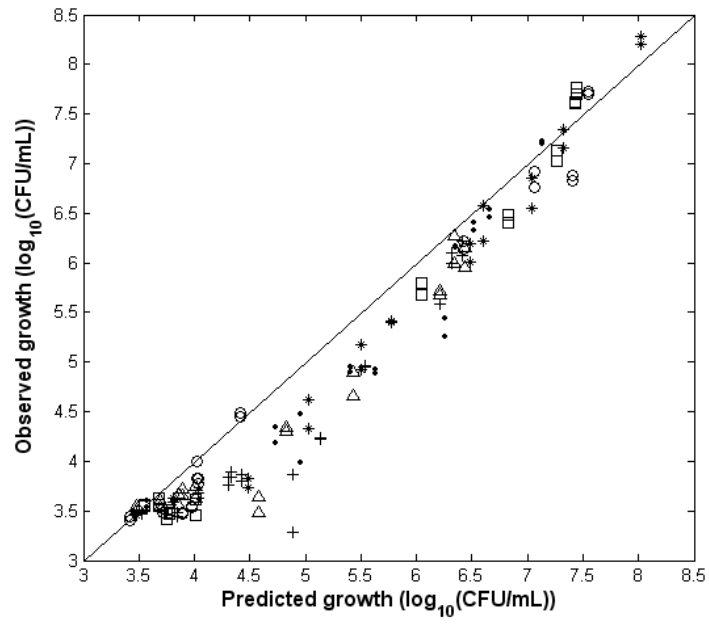
789

790   Fig. 5.

791
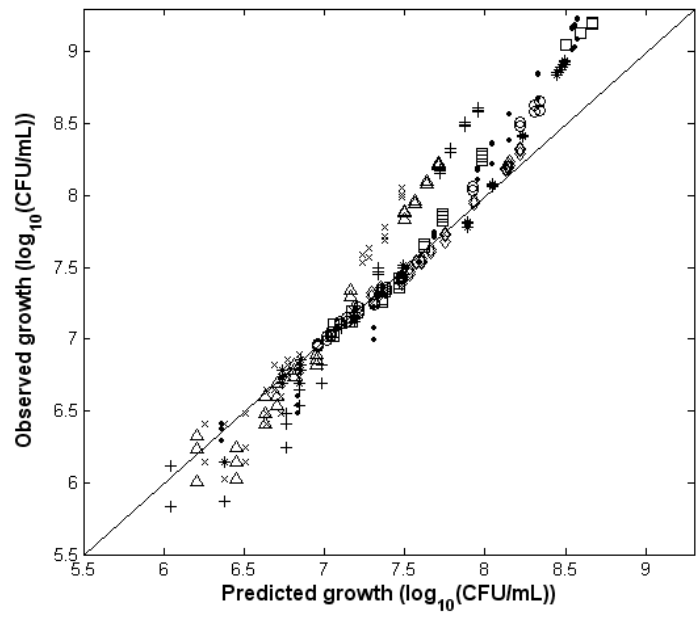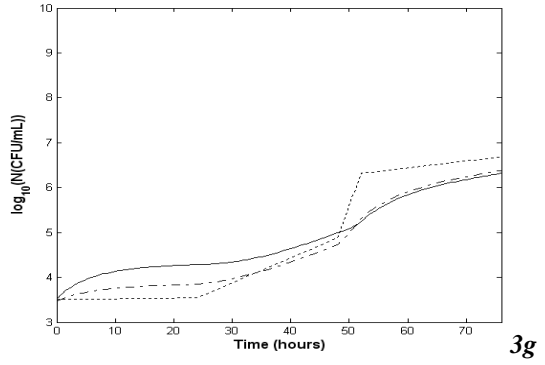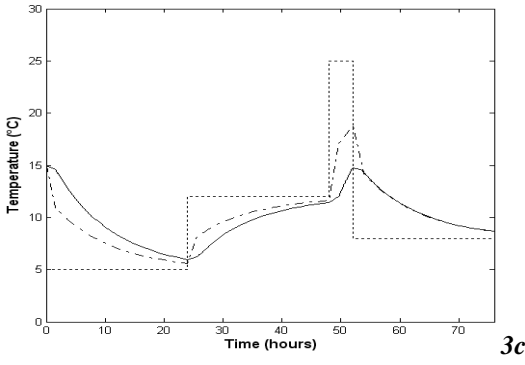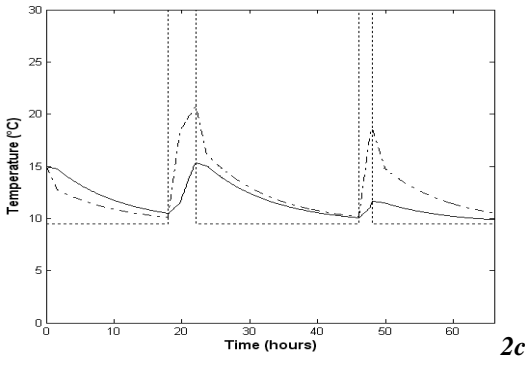
Fig. 6.
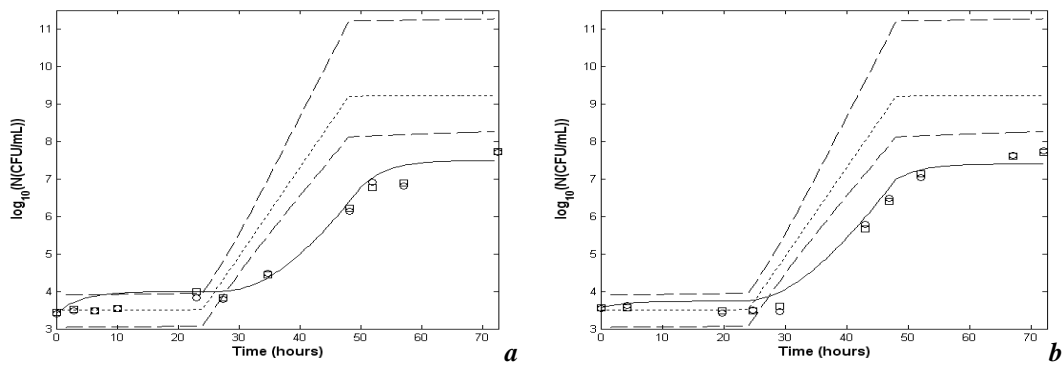
Fig. 7.

796

797 Fig. 8.

798

799

800

801   Fig. 9.

802

803   Table 1

804   List of previous works dealing with models predicting the bacterial growth under dynamic

805   temperature conditions

806

y Model	Secondary model	Solution method	Validation conditions	R
nd Roberts aranyi and 4).	Quadratic polynomial model.	Numerical solution by the fourth order Runge–Kutta method.	Rates of change of T ranging from $1.7°C.h^{-1}$ to a virtually instantaneous change: cooling from 25°C to -2, 2, 5 or 10°C and heating from 2°C to 25°C.	Bovil
gistic model.	Arrhenius equation.	Numerical solution by the fourth order Runge–Kutta method.	Various types of a dynamic temperature history with various intervals were studied for of *Escherichia coli* 1952 growth prediction.	Fujika 2004
nd Roberts aranyi and 4).	A modified Ratkowsky equation (Zwietering et al., 1991).	Numerical solution by the fourth order Runge–Kutta method.	Growth of *Salmonella Enteritidis* in egg yolk under varying temperature profiles (exponential and linear cooling, exponential heating and sinusoidal temperatures).	Gumu al., 20
form of the odel (Gibson	A modified Ratkowsky equation (Zwietering et al., 1991).	Numerical solution by the fourth order Runge–Kutta method.	Growth of *Clostridium perfringens* in cooked ground beef under fluctuating temperature conditions between 30°C and 45°C (square waved) and under continuous temperature changes from 51°C to 10°C (linear and exponential cooling).	Huan

807   Table 2

808   Tested temperature scenarios for the validation of the model at changing air temperature and

809   constant convective heat transfer coefficient equals to 8 $W/(m^2.K)$

810

Stage of the cycle	Temperature (°C)	Duration (h)
Cycle N° 1		
Storage in a cold room	2.5	24
Refrigeration stopped due to an accidental failure of the installation	21	24
Repaired breakdown and remaining product in the cold room	2.5	24
Cycle N° 2		
Industrial storage and transport	9.5	18
Household doorstep delivery	30	4
Storage in refrigerator	9.5	24
Product on the table	30	2
Remaining product in the refrigerator	9.5	18
Cycle N° 3		
Storage and transport	5	24
Storage in the refrigerated cabinet	12	24
Household doorstep delivery	25	4
Storage in refrigerator	8	24

811   Table 3

812   Statistical criteria related to the data of validation at constant air temperature and changing

813   convective heat transfer coefficient

814

Test conditions	R	B_f	A_f
Case 1	0.996	0.98	1.03
Case 2	0.996	0.99	1.01
Case 3 at product centre	0.987	0.98	1.04
Case 3 at product surface	0.987	0.99	1.02
Case 4 at product centre	0.976	0.99	1.05
Case 4 at product surface	0.986	0.99	1.03
Case 5 at product centre	0.975	0.99	1.03
Case 5 at product surface	0.994	1	1.01

815

816

817   Table 4

818   Statistical criteria related to the data of validation at changing air temperature and constant

819   convective heat transfer coefficient equals to 8 W/(m^2.K)

820

Test conditions	R	B_f	A_f
Cycle 1 at product centre	0.991	1.05	1.05
Cycle 1 at product surface	0.992	1.04	1.05
Cycle 2 at product centre	0.963	1.08	1.08
Cycle 2 at product surface	0.986	1.06	1.06
Cycle 3 at product centre	0.944	1.13	1.13
Cycle 3 at product surface	0.964	1.09	1.09

821

822

823